HIGH ACCURACY DEFORMATION MONITORING
OF SPACE STRUCTURES BY HEURISTIC SIMULATION

Jafar Amiri Parian (1), Armin Gruen (1), Alessandro Cozzani (2)
(1) Institute of Geodesy and Photogrammetry
Swiss Federal Institute of Technology Zurich (ETHZ)
(2) European Space Technology and Research Center (ESTEC)
Email: (amiriparian, agruen)@geod.baug.ethz.ch
alessandro.cozzani@esa.int

Abstract: The ESA deep space Planck mission will collect and characterise radiation from the cosmic microwave background using sensitive radio receivers operating at extremely low temperatures. Planck's objective is to analyze, with the highest accuracy ever achieved, the remnants of the radiation that filled the universe immediately after the Big Bang, which we observe today as the cosmic microwave background. To achieve this aim well-manufactured reflectors are used as parts of the Planck telescope receiving system. The system consists of the secondary and primary reflectors which are sections of two different ellipsoids of revolution with mean diameters of 1 and 1.6 meters. Deformations of the reflectors which influence the optical parameters and the gain of receiving signals are investigated in vacuum and at low temperatures. For these investigations, among the high accuracy measurement techniques, photogrammetry was selected. With respect to the photogrammetric measurements, special considerations should be taken into account in different steps of design and processing, such as the determinability of additional parameters under the given network configuration, datum definition, reliability and precision issues as well as workspace limits and propagating errors from different sources of errors. We have designed an optimal close-range photogrammetric network by heuristic simulation for the secondary reflector with a relative precision better than 1:400'000 to achieve the requested accuracies. A least squares best fit ellipsoid was developed to determine the optical parameters of the reflector. In this paper we will report about our procedure, network design and results of real measurements and 3D deformation analysis for the determination of stable monitoring points based on the test executed by Alcatel Alenia Space under ESA-ESTEC contract in vacuum and under very low temperatures.

1. Introduction

The Planck telescope was selected as the third Medium-Sized Mission (M3) of ESA's Horizon 2000 scientific program, and is today a part of its Cosmic Vision program. It is designed to image the anisotropies of the cosmic background radiation field over the whole sky, with unprecedented sensitivity and angular resolution. Planck will help provide answers to one of the most important questions asked in modern science - how did the universe begin, how did it evolve to the state we observe today, and how will it continue to develop in the future? Planck's objective is to analyze, with the highest accuracy ever achieved, the remnants of the radiation that filled the universe immediately after the Big Bang, which we observe today as the Cosmic Microwave Background (CMB). The Planck mission will collect and characterise

radiation from CMB using sensitive radio receivers operating at extremely low temperatures. These receivers will determine the black body equivalent temperature of the background radiation and will be capable of distinguishing temperature variations of about one micro-Kelvin. These measurements will be used to produce the best ever maps of anisotropies in the CMB radiation field.

To achieve this aim well-manufactured reflectors are used as a part of the Planck telescope receiving system (Figure 1). The telescope consists of a Secondary Reflector (SR) and a Primary Reflector (PR) which are specific sections of two different ellipsoids of revolution with mean aperture size of 1 meter and 1.6 meters. Deformations of the reflectors, which influence the optical parameters and the gain of receiving signals, are investigated in vacuum and at low temperatures (down to 95 Kelvin) to investigate the correlation of the thermoelastic model used in its design with respect to the actual performance. Surface accuracy and optical parameters (radius of curvature and conic constant) and their precisions are requested parameters defined by ESA-ESTEC[*].

For the deformation monitoring the concept of hyper-image digital photogrammetry was used. This is base on extremely high network redundancy and the modeling of all possible systematic errors. We report in this paper about the simulations and real measurements of the SR only.
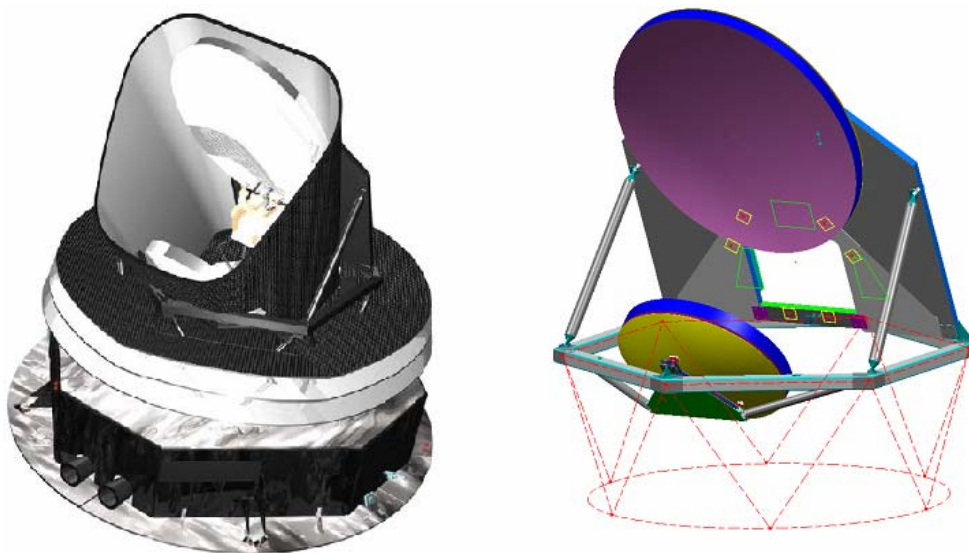

Figure 1. Planck Telescope. Receiving system with the Primary (top) and the Secondary (bottom) Reflectors (Courtesy of Alcatel Alenia Space).

For the sake of simplicity this problem was divided into three sub-problems according to the concept of the network design that was proposed by Grafarend [9]:

1) Second Order Design (SOD)

> To relate the point coordinates to the optical parameters of the reflectors, a best fit ellipsoid method was developed and based on it, SOD was performed to determine the required precision of the point coordinates with respect to the requested optical parameters.

---

[*] http://www.esa.int/esaCP/SEMOMQ374OD_index_0.html

2) First Order Design (FOD)

> A close-range photogrammetric network was designed by heuristic simulation in order to achieve the precisions of the point coordinates which were estimated in the previous step.

3) Zero Order Design (ZOD)

> Selecting an appropriate datum in order to achieve the best possible precision of the optical parameters.

Based on the designed photogrammetric network a real test was executed by Alcatel Alenia Space[*] for the measurement of the SR and evaluation of its deformation in vacuum and at very cold temperatures.

2. Best Fit Ellipsoid and Second Order Design

The SR is a section of an ellipsoid of revolution around a Z-axis with a and b as principal axes (Equation 1).

$$\frac{X^2}{b^2} + \frac{Y^2}{b^2} + \frac{Z^2}{a^2} = 1 \tag{1}$$

The optical parameters of SR are computed by equations (2) and (3):

$$K = E^2, \text{ with } E^2 = 1 - \frac{b^2}{a^2} \tag{2}$$

$$R = a(1 - E^2) \tag{3}$$

In which K, R and E are the conic constant, the radius of curvature and the eccentricity.

Equation (1) is a standard form of an ellipsoid of revolution with aligned principal axes to the axes of the coordinate system and the ellipsoid center at the origin. In the case of a different coordinate system of the point cloud with respect to the coordinate system of the ellipsoid, an appropriate transformation is used for mapping the point cloud to the ellipsoid coordinate system.

The solution is acquired by selecting a suitable optimization method for the registration of the point cloud to the standard ellipsoid (Equation 1). The optimization method is based on least squares and is similar to the method which was already proposed for markerless registration of point clouds by Gruen and Akca [12].

The requested accuracies are related to the optical parameters of the SR which were defined by ESA-ESTEC. These parameters cannot be measured directly with photogrammetry. Therefore points on the surface of the SR are measured and the optical parameters are estimated using the mentioned best fit ellipsoid method. These points in our case are the center of circular retro-reflective targets.

The distribution of targets, the number and precision of the point coordinates are the factors that influence the precision of the optical parameters. Since the SR is a section of an ellipsoid it has different curvatures in different areas. Therefore the targets have to be distributed such that there exist a sufficient number in areas of higher curvature. In addition, the increase of

---

[*] http://www.alcatel.com/space/index.htm

the number of points increases the precision of the optical parameters. The precision of the 3D points is also another factor influencing the precision of the optical parameters.

Since the configuration is known, the problem in this step is to decide the weights of the observations (point coordinates) to meet design criteria. The precision values of the observations are estimated by SOD. In other words, the weight matrix of observations, which are X, Y and Z coordinates, are estimated from the covariance matrix of unknowns, which are the optical parameters. The weight matrix computed from SOD is not diagonal. However, for strong geometrical networks with a relatively large number of targets, it can be assumed that this weight matrix is a diagonal matrix. To be sure that the diagonal weight matrix, which is constructed by the estimated precision of the point coordinates from SOD is fulfilling the requirements, an error propagation was done to estimate the precision of the optical parameters.

In addition, the target thickness and the ambiguity of target thickness were modeled in the best fit ellipsoid for the error propagation. Considering the potential accuracy of the photogrammetric method and possible number of targets that could be sticked on the surface of the SR, successful results were achieved by using approximately 450 targets that were distributed homogeneously on the surface of the SR. A homogeneous distribution of targets makes target sticking easier and needs less effort with respect to other target maps (inhomogeneous distributions).

3. Close-range Photogrammetric Network Design by Heuristic Simulation

Previous research on this topic in close-range photogrammetry was done by Fritsch and Crosilla [8], who performed first order design with an analytical method. Fraser [4, 5, 6] discussed the network design problem in close-range photogrammetry. Mason [14] used expert systems and Olague [15] used a genetic algorithm for the placement of matrix array cameras using heuristic computer simulations. Precision and reliability considerations in close-range photogrammetry, as a part of the network quality requirements, have been addressed by Gruen [10, 11] and Torlegard [16]. Considerations on camera placement for the determination of the additional parameters of the camera by using control points were addressed by Gruen and Beyer [13]. The relation between highly redundant image acquisition and the respectively very high accuracy in point coordinates was already demonstrated by Amiri Parian [1] and Fraser et al. [7].

The aim of heuristic simulation is to design an optimal close-range photogrammetric network with a precision which matches the required values from the previous step of SOD. In addition to the work space limits and existing facilities for the placement and orientation of the camera the network should also be able to:

a) de-correlate the point coordinates with respect to the other parameters (the exterior orientation and additional parameters of the camera).

b) estimate additional parameters reliably

c) reduce the photogrammetric block triangulation error caused by the incidence angle of retro-reflective targets (reflectivity).

d) reduce the error of image target center (eccentricity) by selecting an appropriate location and orientation of the camera and a suitable target size. The image target center error is the error of the measured target center with respect to the physical target center because of the perspective projection effect of the target.
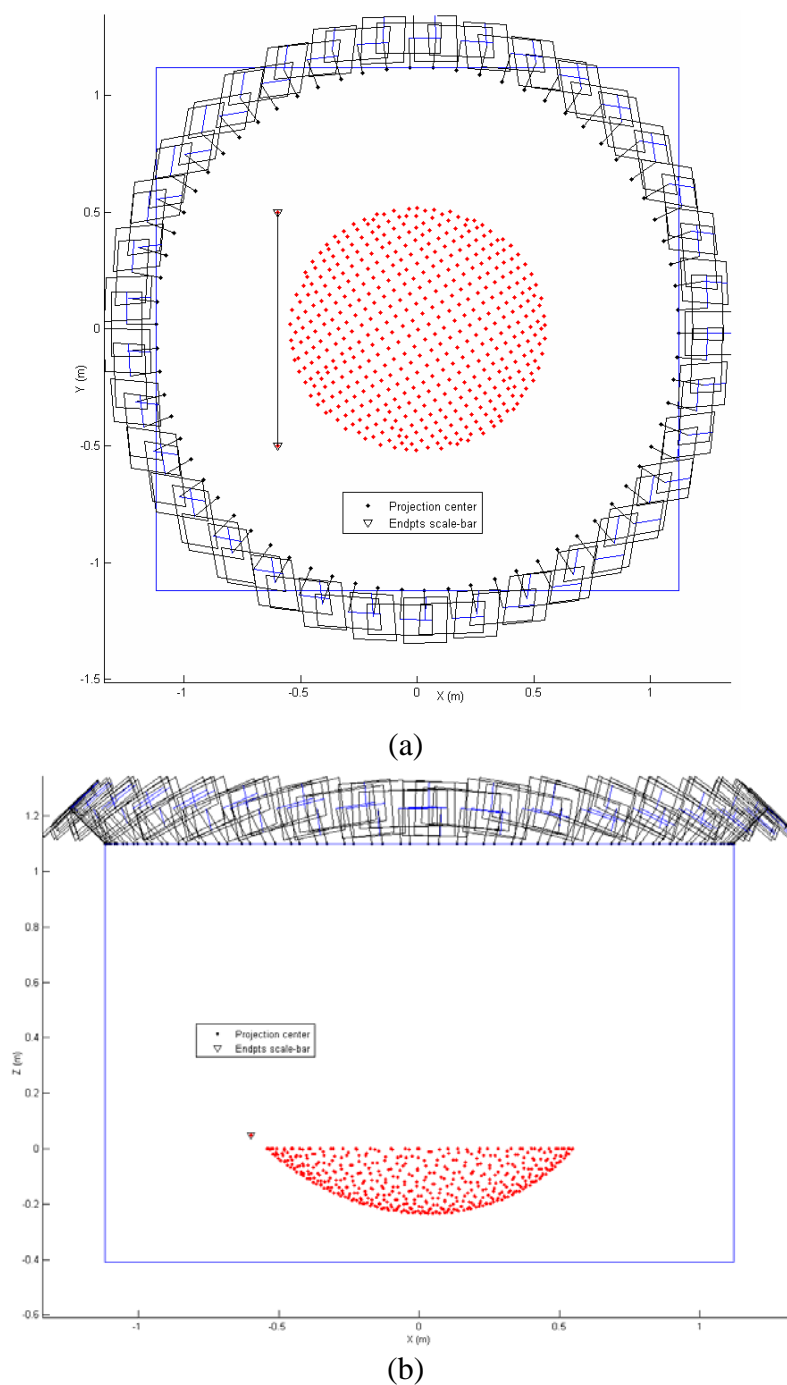
(a)

(b)

Figure 2. Network configuration. (a) XY-view (aperture of SR) and scale-bar at the left side (b) XZ-view of the network.

Considering the existing facilities of Alcatel Alenia Space (with the capability to operate at very cold temperatures) a network was designed that satisfies the above 4 conditions.

Figure 2 shows the configuration of the camera stations with respect to the SR. The network consists of 70 stations with 1 image per station. The incidence angle of the camera with respect to the aperture of the SR is 45 degrees. With the assumption that the internal accuracy of the camera system is 0.02 pixel the relative precision of the network is better than 1:400' 000.

4. Datum Definition

For an accurate estimation of the optical parameters appropriate datums were selected. Two datum choices were used for the estimation of these parameters:

1. An inner constraints datum for resolving 7 datum defects

2. With a known distance, an inner constraints datum for resolving the remaining 6 other datum defects

An inner constraints datum for resolving 7 datum defects is the best datum for the estimation of the conic constant because this parameter is scale-independent.

The first datum cannot be used for the estimation of radius of curvature because this parameter is scale-dependent. The scale is defined by a scale-bar with a known distance and its uncertainty. This distance is used as an observation in the adjustment and an inner constraints datum is used for resolving the remaining 6 other defects of the datum.

5. Results of Real Measurements

Real measurements according to the designed network were executed by Alcatel Alenia Space under ESA-ESTEC contract. A 6-megapixel commercial camera was used in the test. Before measuring the Planck Primary and Secondary Flight Models (PRFM and SRFM respectively), the Qualification Model of the Planck Secondary Reflector (SRQM) was measured in vacuum and at temperatures down to 95 Kelvin, in total at 13 epochs.

The extremely high accuracy could be achieved by highly redundant image acquisition. In the average 68 images were acquired in each epoch, overlapping all each other. In addition, to avoid systematic errors caused by the eccentricity of the target center in object space, the rays with incidence angle greater than a criterion which was computed in the design step were not used in the computations. Blunder detection was done automatically using a dynamic threshold based on RMS values of image point residuals. To compensate for systematic image errors Brown's additional parameters (APs) set (Gruen and Beyer [13]) with 10 APs were applied. They all turned out to be significant, causing a maximum systematic deformation in image space of 79 pixels.

We used our own bundle adjustment software for the processing of the observations. The global redundancy for the system was 0.95 and the RMS value of the image point residuals from bundle adjustment was 0.12 micron which correspond to 1/70 pixel. The mean standard deviations of the XY (σ_{XY}) and Z coordinates (σ_Z) of the object points were 4 and 3 microns respectively with the maximum of 5 and 4 microns.

To investigate target stability in vacuum and cold temperatures, 6 different types of targets with different reflective and adhesion parts were used in the test by ESA-ESTEC. Table 1 summarizes this information and shows the number of available targets in each epoch which were counted based on image point measurements. Unexpectedly many targets were unstable, displaced and fell off. Therefore the data reduction of epochs M03 to M09 was complicated. The main problems of these epochs were:

1) instability of targets during image acquisition

2) determination of surface deformation of the SRQM from the displaced targets because of losing the adhesion at very cold temperatures

These two problems were solved to retrieve optical parameters in epochs M03_1 and M04. The first problem was solved by dividing the network into sub-networks in each of which targets were stable and bundle adjustment could be done successfully. The second problem was solved by 3D deformation analysis of the very cold epochs with respect to one of the ambient epochs.

The relative precision of the real network is in a good agreement with the simulated network and is better than 1: 400'000. By choosing an appropriate datum, the optical parameters were estimated by the developed best fit ellipsoid (for the shaded epochs in Table 1) and the results are in the range of specifications that were defined by ESA-ESTEC.

Table1. Number of existing targets in each epoch (counted based on image point measurements).

#	Epoch	Temperature (Kelvin)	Pressure	Target type					
				ESA	Alcatel	W_ESA	K_Alcatel	P_Alcatel1	K_ESA
1	M00	ambient	ambient	471	58	7	13	7	9
2	M01	ambient	ambient	471	58	7	13	7	9
3	M02	ambient	vacuum	471	58	7	13	7	9
4	M03	140	vacuum	219	58	7	13	7	9
5	M03_1	110	vacuum	217	39	7	13	7	9
6	M04	95	vacuum	217	34	2	13	6	9
7	M05	200	vacuum	217	34	2	13	6	9
8	M06	170	vacuum	217	34	2	13	6	9
9	M07	140	vacuum	218	33	2	13	6	9
10	M08	100	vacuum	217	31	2	13	6	9
11	M09	230	vacuum	197	26	2	13	6	9
12	M10	ambient	vacuum	202	31	2	13	6	9
13	M11	ambient	ambient	204	31	2	13	6	9

5.1. Instability of targets during image acquisition

Figure 3 shows an example of the displaced targets of epoch M03_1 with respect to the location of targets at epoch M01. The gap of stations at the left side is due to the restriction of the mechanical instrument for the implementation of the network. The instability of targets during image acquisition in this epoch was realized after analyzing datum independent parameters of the network. In this case datum independent parameters are a posteriori standard deviation ($\hat{\sigma}_0$) and APs of the camera. It can be proved that if the network configuration does not change then $\hat{\sigma}_0$ and APs do not change for all minimal constraints datum. In epoch M03_1, with 110 Kelvin temperature, the estimated APs from bundle adjustment and $\hat{\sigma}_0$ are much different than the APs and $\hat{\sigma}_0$ from previous successful processed epochs (M00, M01, M02). Since the network configuration of this epoch is the same as in previous epochs the reason of such difference could be explained by:

a) Instability of the camera due to low temperature and change of APs

b) Target displacement during the image acquisition

The first hypothesis was investigated by Alcatel Alenia Space and ESA-ESTEC. Since the camera was inside a canister and the temperature was stable with approximately ambient temperature this hypothesis was rejected. Therefore we investigated the second hypothesis.

Considering the image acquisition time that was approximately one hour for each epoch (67-69 stations) a target displacement could have happened because of the different gradient of temperature on the surface of SRQM and loss of target adhesion in cold temperature. With the assumption that the targets were stable for a short time, the network was divided into sub-networks. For that photogrammetric block triangulation was started with three images. Then successively according to the sequence of the image acquisition, images were added to the current sub-network. This addition was continued until APs and $\hat{\sigma}_0$ did not change significantly. After construction of the first sub-network in which targets were stable, other sub-networks were constructed in the same way by the remaining images. At the end, several sub-networks were constructed in a way that each sub-network has its stable targets. By searching for common points in successive sub-networks and growing the sub-networks in the same manner a network was constructed which consisted of the stable targets only.
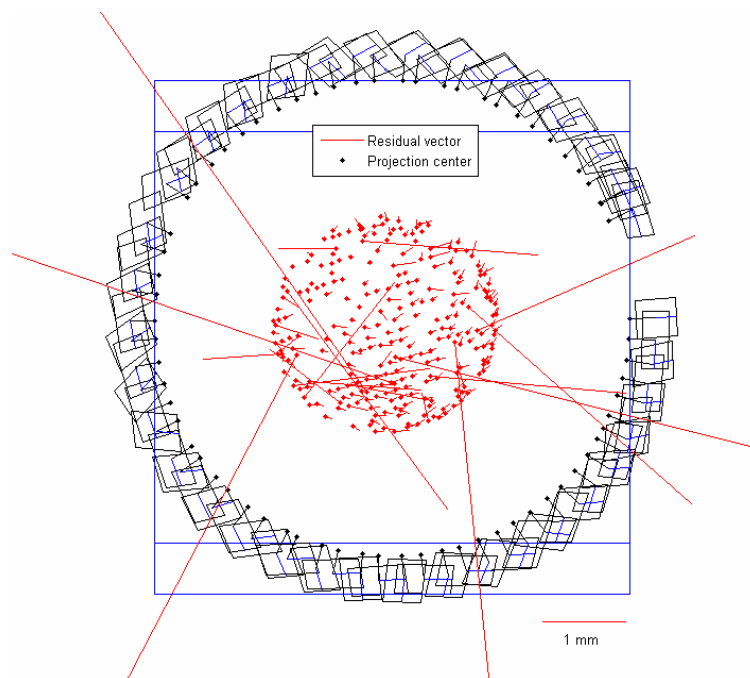

Figure 3. Target displacement and surface deformation of epoch M03_1 with respect to epoch M01.

5.2. Determination of surface deformation of SRQM from target displacement

After successful determination of the stable targets the next step is to determine the SRQM deformation from target displacements. For the sake of simplicity, we assumed that the SRQM at epoch M03_1 does not have any relative deformation with respect to the SRQM at M01. By this assumption deformation analysis was done by the congruency testing method proposed in Chen [3] and Caspary [2].

The maximum deformation of the composite material (SRQM) at cold temperatures which was estimated by a thermoelastic model was used as maximum probable deformation of the surface itself. In other words, any deformation greater than this value is assumed to be target displacement. By the stable points, which were detected from deformation analysis, an inner

constraints datum was defined and any displacement vector which was smaller than a predicted value from thermoelastic model, was assumed to be a deformation of the SRQM. Figure 4 shows the estimated stable targets (58 targets) of epoch M03_1 after this procedure. This procedure was applied for epoch M04 and the number of detected stable targets was 35. This procedure was applied for epoch M08 but the results were not satisfactory and not successful. The reason could be that the signal to noise ratio was small in this epoch.
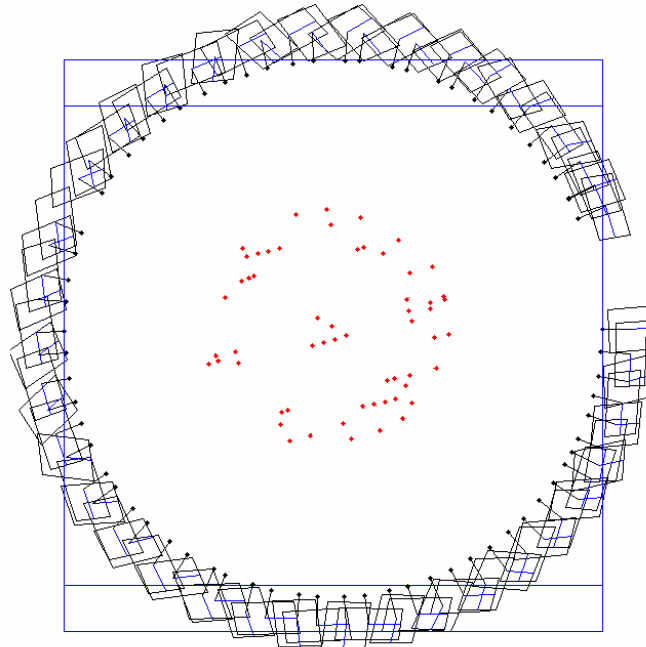

Figure 4. New network configuration after detecting stable targets and deformation analysis.

6. Conclusions

Three steps of network design: SOD, FOD and ZOD were performed. In SOD the precision of the point coordinates was estimated from the requested precision of the optical parameters. A least squares surface modeling for ellipsoid fitting was developed based on the given model of the reflector to relate the point coordinates with optical parameters. FOD was performed by heuristic simulation to find an optimal configuration of camera stations in order to achieve the estimated precision of the point coordinates in the previous design step (SOD). ZOD was performed in order to achieve the best possible precision of the optical parameters. An optimal close-range photogrammetric network was designed by heuristic simulation with a relative precision better than 1: 400'000.

A real measurement of the SRQM was performed based on the designed network by Alcatel Alenia Space under ESA-ESTEC contract at 13 epochs with a coldest temperature at 95 Kelvin. The RMS residuals were 0.12 micron and the mean object point precision was 4 and 3 microns for the lateral and depth axes. This extremely high precision could be acquired by a strong geometrical network, the concept of hyper-redundancy, efficient blunder detection method, advanced self-calibration and considering target center eccentricities.

At low temperature epochs many targets were unstable, displaced and fell off because of the loss of target adhesion. To detect stable targets in each epoch, the network was divided into sub-networks and sub-networks were merged together in a way that the new network contains only the stable targets. A deformation analysis was performed to detect displaced targets with respect to the first epoch. The target displacement because of loss of target adhesion was

filtered from the surface deformation using a maximal probable surface deformation of the thermoelastic model. The results from this measurement are in a good agreement with respect to the designed values and the accuracies are in the range of the specifications.

This measurement of the Planck SRQM validated the network design and demonstrated its robustness even when confronted with major target loss. This paved the way for the successful use of much denser but similarly-designed networks for the measurements of the Planck Secondary Reflector Flight Model and of the Planck Primary Reflector Flight Model, both performed later in the same Alcatel Alenia Space facility.

Acknowledgements

References

[1]   Amiri Parian J.: Close-range Photogrammetric Network Design Based on Micro-Cameras for Herschel Spacecraft. Technical report for ESA-ESTEC, November, 2004.
[2]   Caspary, W. F.: Concept of Network and Deformation Analysis. School of Surveying, The University of New South Wales, Monograph 11, 1987.
[3]   Chen, Y. Q.: Analysis of deformation surveys – A generalized method. Department of Surveying Engineering, Technical Report No. 94, University of New Brunswick, Fredericton, N.B., 1983.
[4]   Fraser, C.: Network Design Considerations for Non-Topographic Photogrammetry. Photogrammetric Engineering and Remote Sensing, Vol. 50, No. 8, August, 1984, pp. 1115-1126.
[5]   Fraser, C.: Photogrammetric Measurement to One Part in a Million, Photogrammetric Engineering and Remote Sensing, Vol. 58, No. 3, March, 1992, pp. 305-310.
[6]   Fraser, C.: Network Design. Chapter 9, Close-range Photogrammetry and Machine Vision, edited by Atkinson, Whittles/Scotland, 1996, pp. 256-281.
[7]   Fraser, C., Woods A., Brizzi D.: Hyper Redundancy for Accuracy Enhancement in Automated Close-range Photogrammetry. The Photogrammetric Record, 20 (111), September, 2005, pp. 205–217.
[8]   Fritsch, D. and Crosilla, F.: First Order Design Strategies for Industrial Photogrammetry, SPIE Vol. 1395: Close-Range Photogrammetry Meets Machine Vision, 1990, pp. 432-438.
[9]   Grafarend, E.: Optimization of Geodetic Networks. Bollentino di Geodesia a Acience Affini, Vol. 33, No. 4, 1974, pp. 351-406.
[10]   Gruen, A.: Accuracy, Reliability and Statistics in Close-Range Photogrammetry. Symposium of ISP, Commission V, Stockholm, August, 1978.
[11]   Gruen, A.: Precision and Reliability Aspects in Close-Range Photogrammetry. XIV Congress of ISP, Commission V, Hamburg, July, 1980.
[12]   Gruen, A. and Akca, D.: Least Squares 3D Surface and Curve Matching. ISPRS Journal of Photogrammetry and Remote Sensing, Vol. 59, No. 3, 2005, pp.151-174.
[13]   Gruen, A. and Beyer, H. A.: Calibration and Orientation of Cameras in Computer Vision, edited by Gruen, A. and Huang, T. S., Springer Series in Information Sciences, 2001.
[14]   Mason, S.: Expert System-Based Design of Photogrammetric Networks. Institute of Geodesy and Photogrammetry, ETH Zurich, Switzerland, PhD Thesis, 1994.
[15]   Olague, G.: Automated Photogrammetric Network Design Using Genetic Algorithms, Photogrammetric Engineering and Remote Sensing, Vol. 68, No. 5, May, 2002, pp. 423-431.
[16]   Torlegard, K.: On Accuracy Improvement in Close-range Photogrammetry. Proceedings of Industrial and Engineering Survey Conference, London, 1980.